March 22, 1988 PFC/JA-88-10

Operation of an E || B End Loss Ion Spectrometer on the Tara Tandem Mirror

J.A. Casey, S.F. Horne, J.H. Irby,
R.S. Post, and E. Sevillano,
M.I.T. Plasma Fusion Center;
and J.H. Foote,
Lawrence Livermore National Laboratory.

An **E** || **B** End Loss Ion Spectrometer (ELIS) from the Livermore TMX-U tandem mirror experiment was installed on Tara for high resolution ion spectroscopy. This diagnostic contains parallel electric and magnetic fields, separating the masses and energies of the ions over 128 collector plates. The ion energy distribution nominally yields confining potentials and parallel ion temperatures. Additional experiments have diagnosed the resonance position of the central cell ion cyclotron heating, RF enhanced losses of high energy sloshing ions in the axicell ("plug"), and observation of MHD instabilities at higher time resolution (20 kHz).

INTRODUCTION:

The open geometry of mirror experiments allows for detailed energy analysis of those particles flowing out of the confinement regions. A conventional gridded end-loss analyzer (ELA) can obtain a single measurement of an endloss ion or electron distribution function in a sweep period (the time to sweep the retarding grid through the dynamic range of the analyzer) with good sensitivity, however the time resolution is limited by the sweep period, and the energy range is limited by the breakdown voltage of the retarding grids.

Recently, two $\mathbf{E} \parallel \mathbf{B}$ end loss ion spectrometers (ELIS) were constructed at Lawrence Livermore National Laboratories[1,2] for the TMX-U experiment. This type of diagnostic, first constructed for charge exchange studies on tokamaks[3] collimates the endloss particles, then drifts them across a constant magnetic field separating ions and electrons by energy and charge/mass ratio. In addition, a uniform electric field parallel to the magnetic field further separates ions by species. This diagnostic has several advantages. First, the ions and electrons are separated spatially by the internal magnetic field, so that energetic electron bursts cannot decrease the ion signal as in gridded analyzers. Second, discrimination of higher energy ions is possible since there are no grids to arc. Third, all energy channels are digitized separately and simultaneously, thus much higher time resolution is possible than with a gridded analyzer. In trade, this device is quite a bit more expensive and cumbersome, and due to the narrow collimating apertures, the sensitivity is lower than that of gridded analyzers by about an order of magnitude. The construction and operation details of the ELIS are described elsewhere[1,2].

One of the TMX-U ELIS diagnostics was installed on the Tara tandem mirror experiment during 1987 to extend the Tara diagnostic set and to compare results with TMX-U. In a similar exchange, the other LLL ELIS was simultaneously installed on the Gamma-10 experiment at Tskuba, Japan[4].

Installation and Calibration:

The Tara ELIS installation duplicated the TMX-U setup as closely

as possible, with two major exceptions. First, the CAMAC crate which housed timing modules and digitizers was located 2–3 meters away from the ELIS in a shielded rack for noise suppression, rather than being mounted directly on the ELIS. Because of the extra distance to the digitizers, the 128 signal cables were lengthened and placed in a flexible shield, without loss of response time. Second, the CAMAC crate was installed on the Tara MDS data acquisition system[5] in order to incorporate the ELIS data into the Tara database quickly and easily. Run-time analysis software was written for the VAX-VMS/MDS environment to process and plot ELIS results along with the rest of the Tara dataset.

The **B** and **E** field settings of the ELIS were calibrated with an *in situ* saddlefield ion source, and found to be identical with the LLL calibrations (within the uncertainties of the measurement), confirming that it is possible to transport a delicate one-ton diagnostic across the country without misalignment occurring.

Initial comparisons of the ELIS distribution function with that of an adjacent gridded ELA yielded agreeable results, as on TMX-U and Gamma-10. Differences (lower ϕ and higher $T_{i\|}$ in the ELIS), are attributable to differences in analysis techniques and the energy resolution of the diagnostics. The comparison of total current collected by the ELIS with that of an adjacent Faraday cup collector was not found to be consistent, however. Attempts to correlate Faraday cup current with adjustable energy weightings of the ELIS spectrum over several hundreds of shots have not yielded satisfactory results.

Results:

The ELIS operated continuously from installation on Tara (June 1987) until the termination of Tara experiments (October 1987). In these runs, only Hydrogen plasmas were used, and the Deuterium detector strip in the ELIS was unnecessary. The speed of the digitizers (LeCroy L8212 32 channel CAMAC modules) restricts data acquisition to a constant value of (rate)×(channels) above 5 kHz; by freeing the Deuterium channels, 10 kHz sampling was possible, providing some resolution of endloss fluctuations on magnetohydrodynamic (MHD) timescales (generally 3-10 kHz). Optionally, 20 kHz or 40 kHz

sampling was used, although the number of active detectors is reduced from 60 to 32 or 16, respectively, at these speeds.

The startup plasma in Tara is heated by central cell ICRH slow waves, launched at a typical mirror ratio of 1.6 (compared to the central cell minimum field)[6,7]. The slow waves propagate into the two minimum field regions in the central cell, and heating occurs at the resonances. The ELIS dramatically shows the effects of scanning the resonance position for this ICRH heating. Figure 1 shows the ELIS energy spectrum at two values of a magnetic field scan in the central cell during ICRF heating while unplugged. Figure 1A shows the spectrum where the ICRF resonance is at the minimum field of the central cell. In this case, the parallel component of the heating is quite low, although the perpendicular temperature (as shown on diamagnetic loops) is high. Figure 1B shows a case where the ICRF resonance has been moved to a mirror ratio of 1.2 (by lowering the central cell minimum field). The heating here is more isotropic, and the central cell potential is decreased, as figure 1C shows.

The ELIS signatures during "plugging" experiments can often be quite deceptive. Figure 2 shows a typical ICRF plugging shot, where ICRF from 20 to 40 msec in one of the axisymmetric plug cells of Tara raises the confining potential by about 100 eV. In this shot, other diagnostics show that the plasma remained stable to MHD oscillations throughout the plugging, and that particle accountability is good (i.e. most of the endloss reduction on the plugged side is accounted for by increased endlosses on the opposite end of the experiment). In contrast, figure 3 shows a shot where ECRH plugging in one axisymmetric plug cell results in loss of MHD stability. The decreased endloss current and increased potential in this case are representative of dramatic MHD oscillations, not plugging, as shown in the drop of central cell density[8].

Losses of energetic ions from axicell neutral beam injection can be associated with Coulomb scattering, or with enhanced loss processes such as microinstabilities or RF diffusion. The ELIS can be used as a diagostic of energetic ion loss by observing the signature of the $E/3$ energy component of the neutral beams in the endloss. In figure 4A, approximately 100 Amps of 20 keV neutral beams were injected at 40°

in the axicell. After scatter into the loss cone (with some drag in the process), the $E/3$ component appears at slightly less than 4 keV as a bump–on–tail in the endloss distribution (shown magnified). By scanning the outer mirror peak magnetic field (see inset), the loss cone angle can be changed, and the high-energy endloss current compared with predictions for Coulomb losses, as in figure 4B.

Similarly, RF diffusion can be observed in the high energy ions with the ELIS. Figure 5 shows the high energy spectrum (from the neutral beam $E/3$ components) with and without plugging ICRF in the axicell.

Summary:

The ELIS has proved to be a flexible and reliable diagnostic. Two ELIS instruments constructed at Lawrence Livermore National Laboratories have been installed and operated on three tandem mirror experiments in the U.S. and Japan with a minimum of difficulty. Baseline operation on the three different experiments has established consistency of analysis and calibration factors. In addition, the differences in experimental configurations have expanded the database of ELIS tandem mirror endloss measurements.

We would like to acknowledge the technical assistance of B.E. Wood and M.D. Brown at Lawrence Livermore National Laboratories, and the engineering design of the support framework for the ELIS on Tara by M. Olmstead. This work was supported by U.S. DOE Contract No. DE-AC02-78ET51013.

References

[1]J.H. Foote, G.W. Coutts, L.R. Pedrotti, L. Schlander, and B.E. Wood, *Rev. Sci. Instrum.* **56,** 1117 (1985)

[2]J.H. Foote, B.E. Wood, M.D. Brown, and G.M. Curnow, *Rev. Sci. Instrum.* **57,** 1786 (1986)

[3]A.L. Roquemore, G. Gammel, G.W. Hammett, R. Kaita, S.S. Medley, *Rev. Sci. Instrum.* **56,** 1120 (1985)

[4]Teruji Cho, James H. Foote, Yousuke Nakashima, Kameo Ishii, Hiroshi Sugawara, Minoru Yokoyama, Tooru Segawa, Takashi Kondoh, Isao Katanuma, Yasuhito Kiwamoto, and Syoichi Miyoshi, *J. Phys. Soc. Japan,* **56,** 3775 (1987)

[5]T.W. Fredian and J.A. Stillerman, *Rev. Sci. Instrum.* **57,** 1907 (1986)

[6]S.N. Golovato, K. Brau, J.A. Casey, J.W. Coleman, M.J. Gerver, W.C. Guss, G.A. Hallock, S.F. Horne, J.H. Irby, R. Kumazawa, J. Kesner, B.G. Lane, J. Machuzak, T.G. Moran, R.C. Myer, R.S. Post, E. Sevillano, D.K. Smith, J.D. Sullivan, R.P. Torti, L. Wang, Y. Yasaka, X.Z. Yao, J.J. Zielinski, submitted to *Phys. Fluids.*

[7]R.S. Post, K. Brau, S. Golovato, E. Sevillano, D.K. Smith, W. Guss, J. Irby, R. Myer, and J. Sullivan, *Nucl. Fus.* **27,** 217 (1987)

[8]J.H. Irby, B.G. Lane, J.A. Casey, K. Brau, S.N. Golovato, W.C. Guss, S.H. Horne, J. Kesner, R.S. Post, E. Sevillano, J.D. Sullivan, and D.K. Smith, *Phys. Fluids* (in press)

Figure Captions

Figure 1. The ELIS energy spectrum (endloss current vs. energy vs. time) is shown for two values of the minimum magnetic field in the Tara central cell for an unplugged plasma. In part **A**, the resonance for central cell ICRH is at a mirror ratio of 1.0, and the heating is quite anisotropic. In part **B**, the resonance has been moved up to a mirror ratio of 1.2 by dropping the minimum field, and the parallel component of the heating increases accordingly as seen in the higher energy endloss. Part **C** shows the dependance of the processed ELIS data, ϕ_{cc} and $T_{i\|}$, on the minimum field.

Figure 2. The ELIS spectrum during ICRF plugging shows a moderate (100 eV) increase in confining potential and corresponding initial drop in endloss current.

Figure 3. The ELIS spectrum during an unstable ECRH plugging shot shows "apparent" plugging — the cutoff potential rises and the endloss current drops. This is due to loss of MHD stability in the central cell, as evidenced by the central cell interferometer signal.

Figure 4. Part **A**: the $E/3$ component of the energetic neutral beam injection shows up (after pitch angle scattering and drag) as a bump-on-tail in the endloss energy spectrum. The inset shows a schematic of the axicell B-field, including the outer plug field variation, neutral beam injection, and ELIS. Part **B**: the ELIS data supports the Coulomb loss model for energetic ions.

Figure 5. Part **A**: the ELIS spectrum shows the scattered $E/3$ neutral beam component in the endloss. Part **B**: with the addition of ICRF in the plug axicell, RF diffusion smears the high energy endloss spectrum.

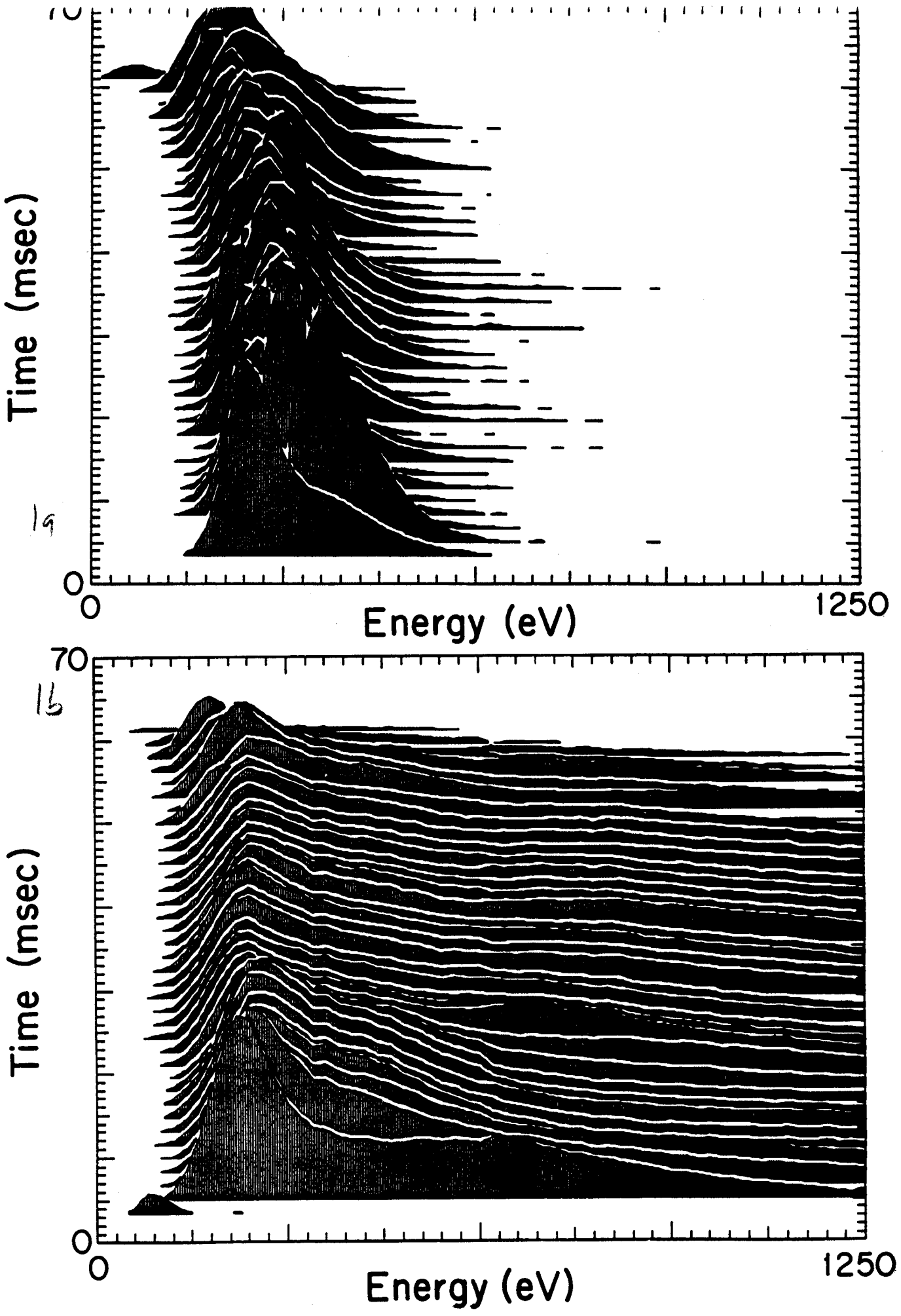
Time (msec)
0
0
Energy (eV)
1250
70
Time (msec)
0
0
Energy (eV)
1250

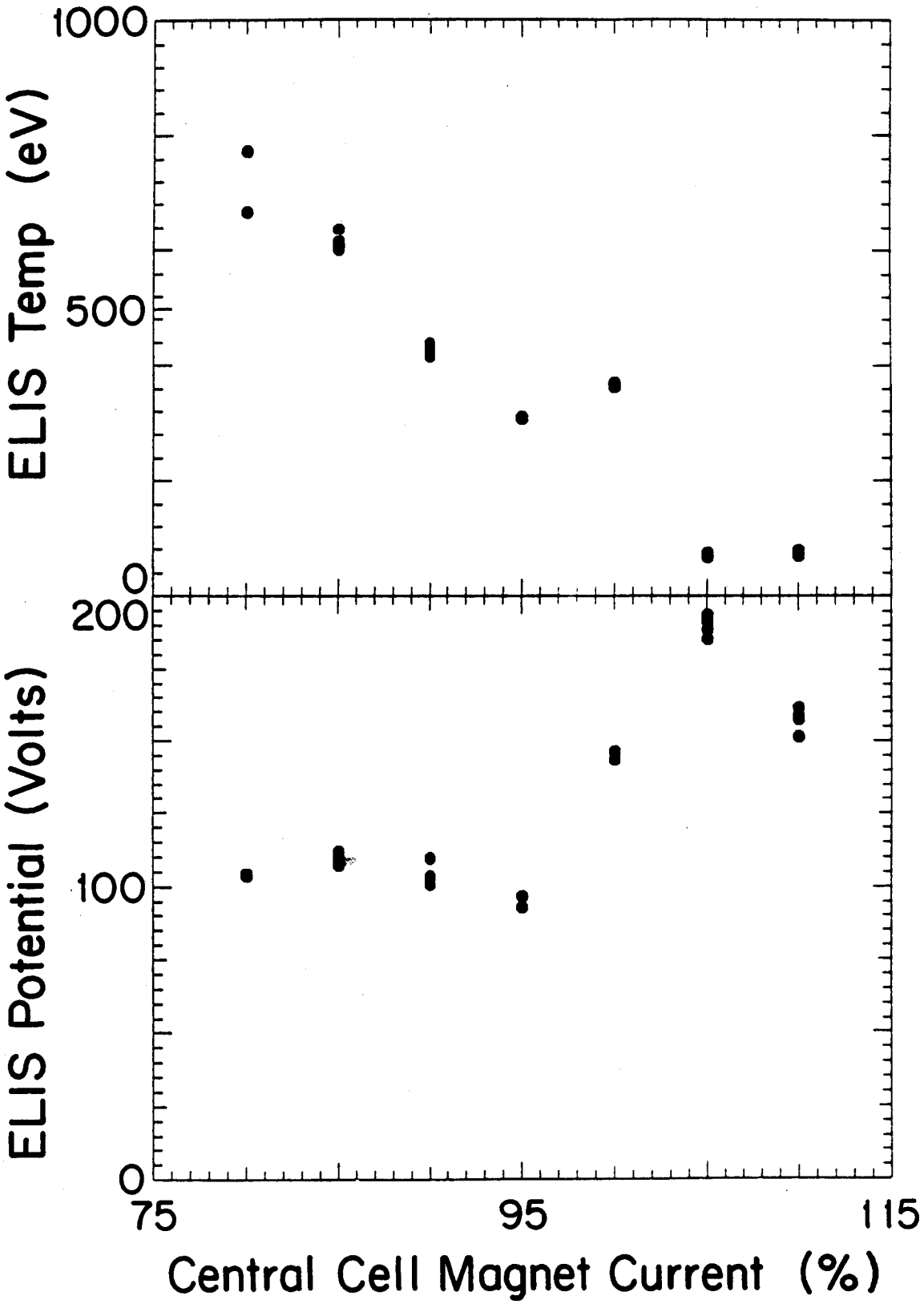
1000
500
0
ELIS Temp (eV)
200
100
0
ELIS Potential (Volts)
75
95
115
Central Cell Magnet Current (%)

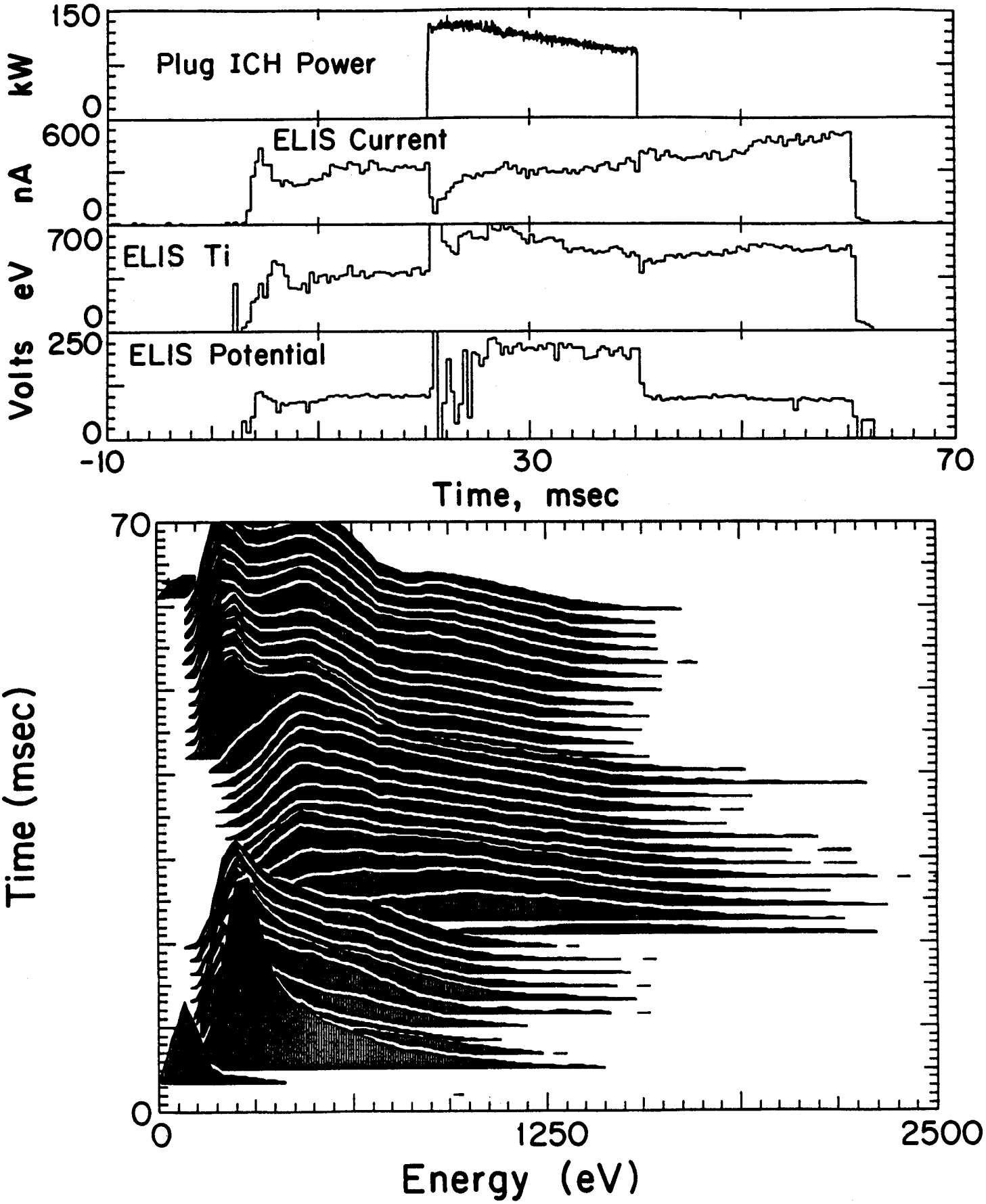
150
0
Plug ICH Power
kW
600
0
ELIS Current
nA
700
0
ELIS Ti
eV
250
0
ELIS Potential
Volts
-10
30
70
Time, msec
70
0
Time (msec)
0
1250
2500
Energy (eV)

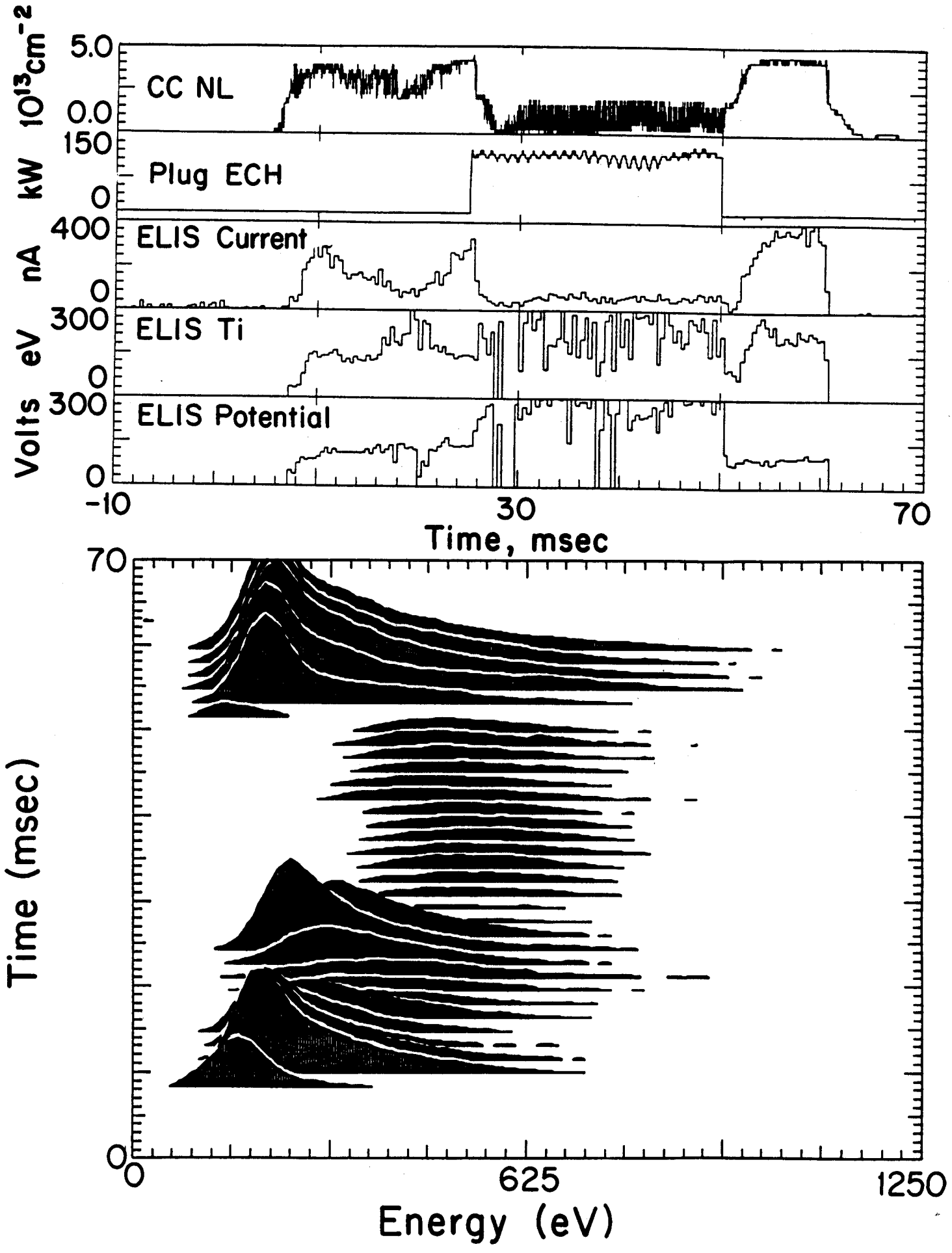
CC NL
Plug ECH
ELIS Current
ELIS Ti
ELIS Potential
Volts eV nA kW $10^{13}cm^{-2}$
5.0
0.0
150
0
400
0
300
0
300
0
-10
30
70
Time, msec
70
0
0
625
1250
Time (msec)
Energy (eV)

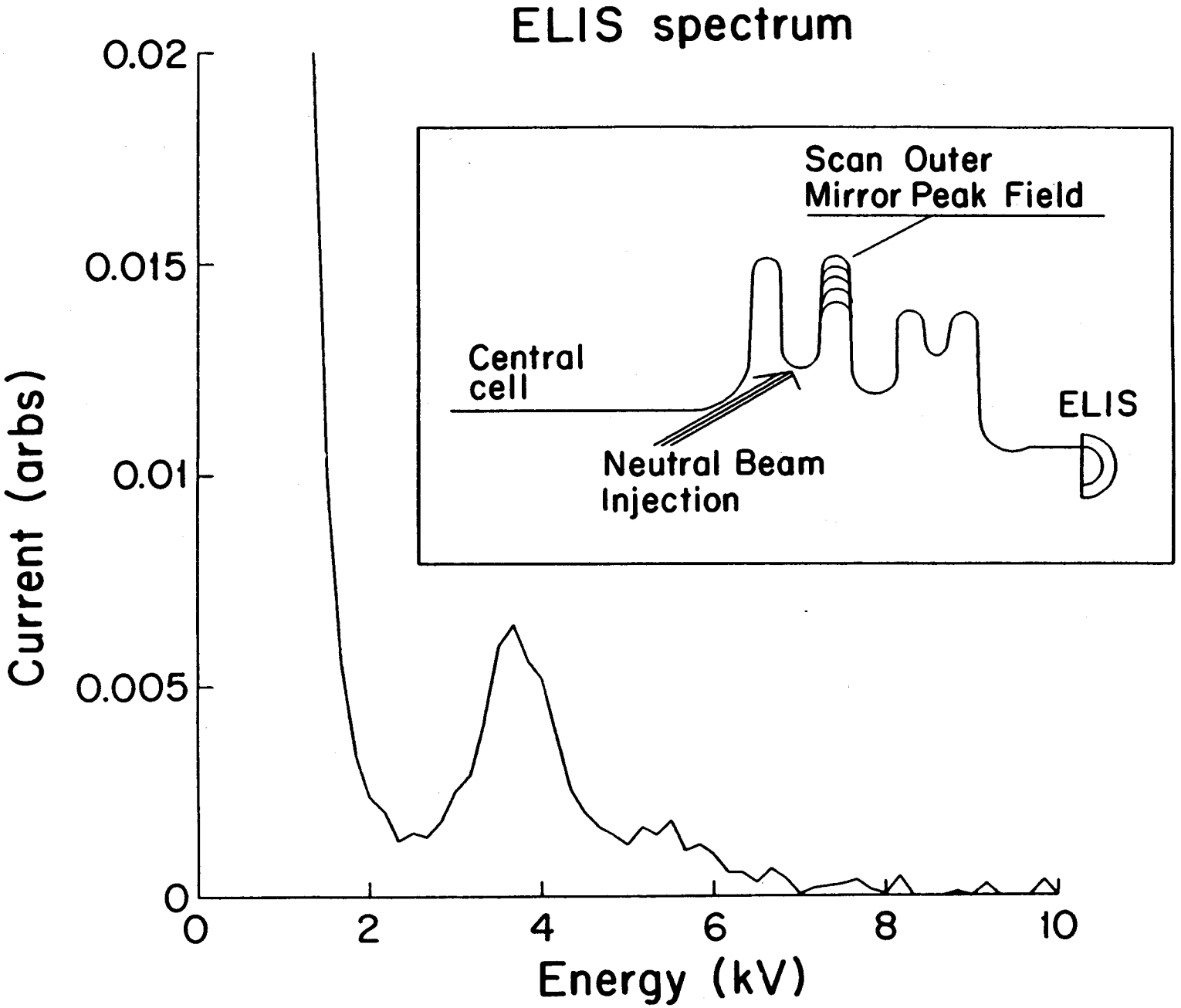
ELIS spectrum
0.02
0.015
0.01
0.005
0
Current (arbs)
0
2
4
6
8
10
Energy (kV)
Scan Outer
Mirror Peak Field
Central
cell
ELIS
Neutral Beam
Injection

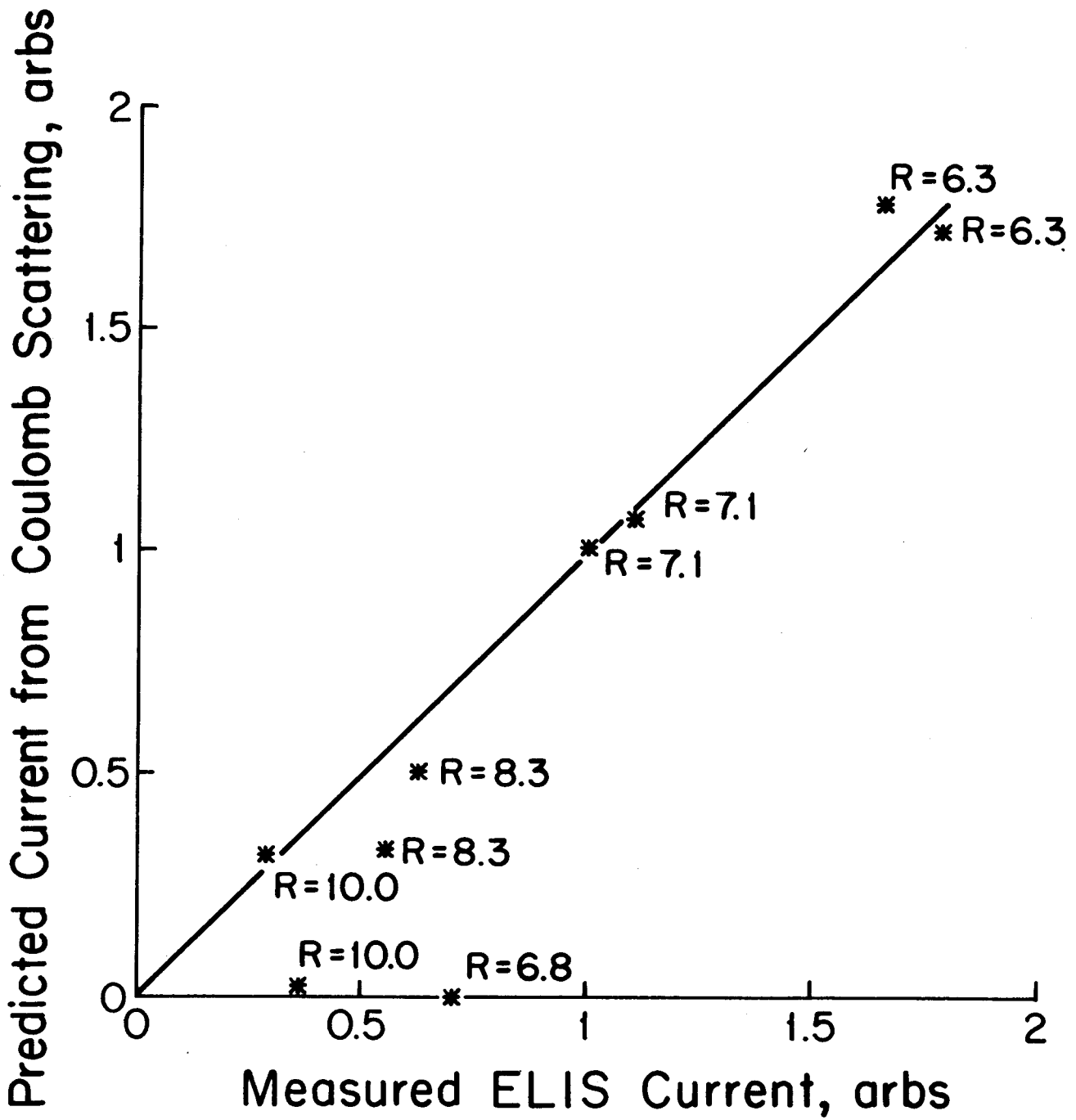
Predicted Current from Coulomb Scattering, arbs
Measured ELIS Current, arbs
0
0.5
1
1.5
2
R=6.3
R=6.3
R=7.1
R=7.1
R=8.3
R=8.3
R=10.0
R=10.0
R=6.8

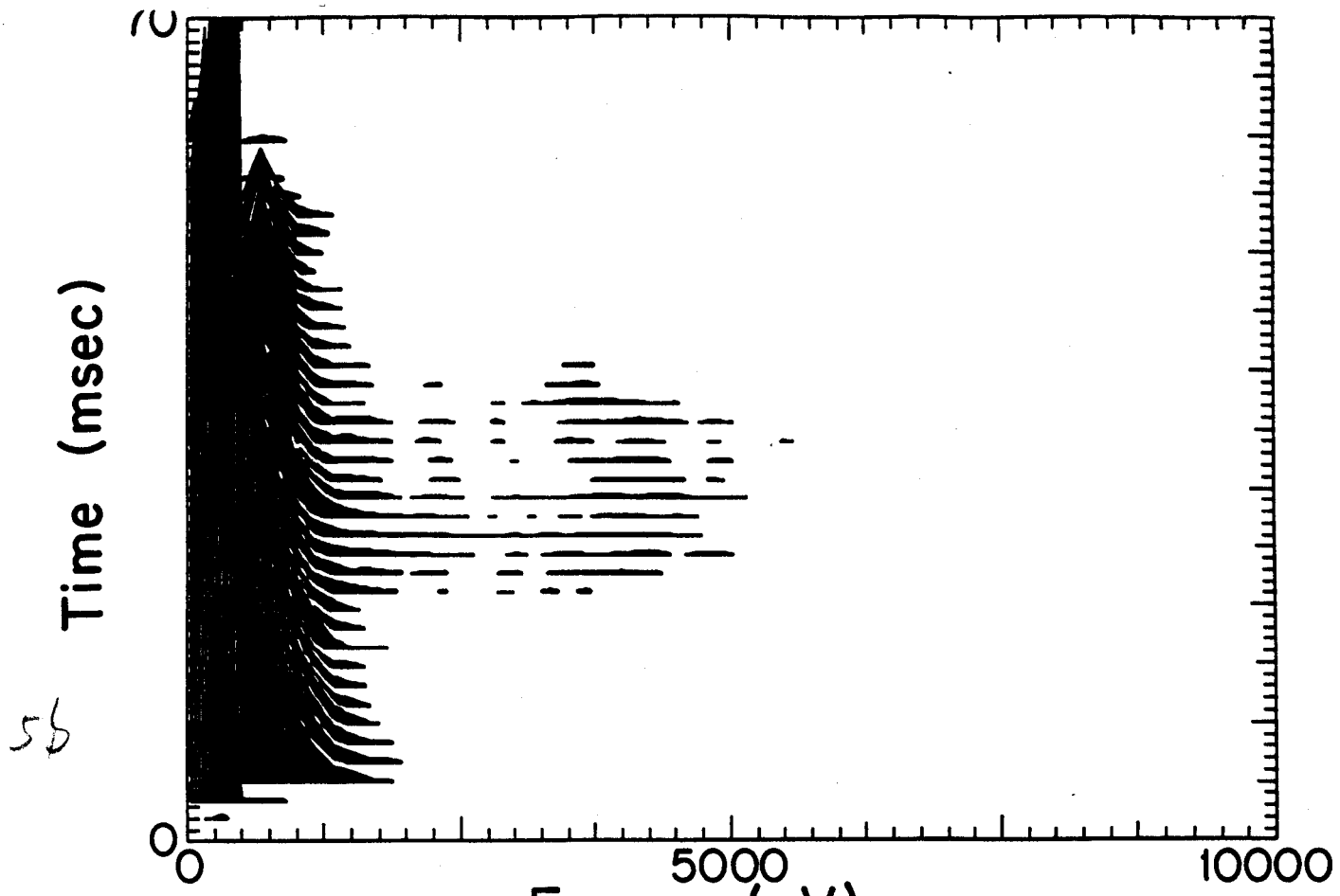
70
Time (msec)
0
0
5000
10000
Energy (eV)

5b

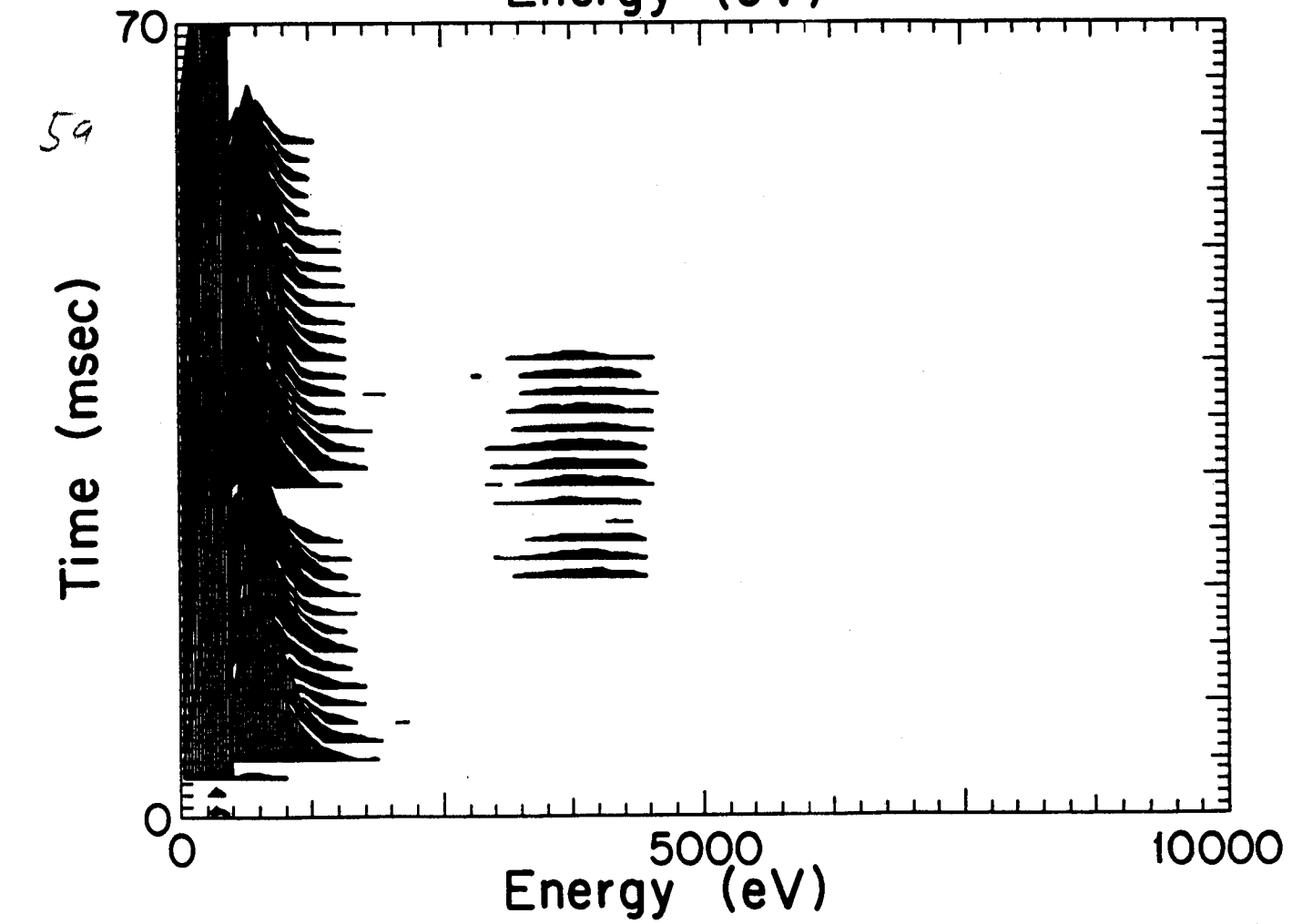
70
Time (msec)
0
0
5000
10000
Energy (eV)

5a